

# Engineered Exosomes Carrying miR-588 for Treatment of Triple Negative Breast Cancer Through Remodeling the Immunosuppressive Microenvironment

Zhengjia Zhang<sup>1,\*</sup>, Xinyi Luo<sup>1,\*</sup>, Xiaoxia Xue<sup>1</sup>, Mingshi Pang<sup>1</sup>, Xiangpeng Wang<sup>1</sup>, Liuchunyang Yu<sup>1</sup>, Jinxiu Qian<sup>1</sup>, Xiaoyu Li<sup>1</sup>, Meng Tian<sup>1</sup>, Aiping Lu<sup>2</sup>, Cheng Lu<sup>3</sup>, Yuanyan Liu<sup>1</sup>

<sup>1</sup>School of Materia Medica, Beijing University of Chinese Medicine, Beijing, People's Republic of China; <sup>2</sup>School of Chinese Medicine, Hong Kong Baptist University, Kowloon, Hongkong, People's Republic of China; <sup>3</sup>Institute of Basic Research in Clinical Medicine, China Academy of Chinese Medical Sciences, Beijing, People's Republic of China

\*These authors contributed equally to this work

Correspondence: Yuanyan Liu; Cheng Lu, Email [yyliu\\_1980@163.com](mailto:yyliu_1980@163.com); [lv\\_cheng0816@163.com](mailto:lv_cheng0816@163.com)

**Background:** The morbidity and mortality of triple-negative breast cancer (TNBC) are still high, causing a heavy medical burden. CCL5, as a chemokine, can be involved in altering the composition of the tumor microenvironment (TME) as well as the immunosuppressive degree, and has become a very promising target for the treatment of TNBC. Dysregulation of microRNAs (miRNAs) in tumor tissues is closely related to tumor progression, and its utilization can be used to achieve therapeutic purposes. Engineered exosomes can avoid the shortcomings of miRNAs and also enhance their targeting and anti-tumor effects through engineering. Therefore, we aimed to create a cRGD-modified exosome for targeted delivery of miR-588 and to investigate its effect in remodeling immunosuppressive TME by anchoring CCL5 in TNBC.

**Methods:** In this study, we loaded miR-588 into exosomes using electroporation and modified it with cRGD using post insertion to obtain cRGD-Exos/miR-588. Transmission electron microscopy (TEM), nanoparticle tracking assay technique (NTA), Western Blots, qPCR, and flow cytometry were applied for its characterization. CCK-8, qPCR and enzyme-linked immunosorbent assay (ELISA), in vivo fluorescence imaging system, immunohistochemistry and H&E staining were used to explore the efficacy as well as the mechanism at the cellular level as well as in subcutaneous graft-tumor nude mouse model.

**Results:** The cRGD-Exos/miR-588 was successfully constructed and had strong TNBC tumor targeting in vitro and in vivo. Meanwhile, it has significant efficacy on TME components affected by CCL5 and the degree of immunosuppression, which can effectively control TNBC with good safety.

**Conclusion:** In this experiment, cRGD-Exos/miR-588 was prepared to remodel immunosuppressive TME by anchoring CCL5, which is affected by the vicious cycle of immune escape. Overall, cRGD-Exos/miR-588 explored the feasibility of targeting TME for the TNBC treatment, and provided a competitive delivery system for the engineered exosomes to deliver miRNAs for antitumor therapy drug.

**Keywords:** engineered exosome, triple negative breast cancer, miR-588, CCL5, tumor environment

## Introduction

Breast cancer is the most common cancer, and the incidence has been increasing in recent years.<sup>1</sup> Triple negative breast cancer (TNBC) accounts for 15–20% of all breast cancers, with strong invasiveness, easy metastasis and poor prognosis.<sup>2</sup> For decades, treatment options for TNBC are very limited, and chemotherapy is always the first-line treatment for patients with TNBC, but treatment efficacy remains unsatisfactory, owing to poor response or intricate immune escape.<sup>3</sup> A growing number of studies have demonstrated that the extensive intra-tumor heterogeneity as well as unique immunosuppressive tumor microenvironment (TME) of TNBC are the main determinants of tumor treatment failure. With the understanding of tumor

immune escape mechanisms continuing to improve, immunotherapy holds promise for the successful control of these malignancies. There is increasing evidence indicating that immunosuppression due to overexpression of certain chemokines and inhibition of immune cells in a depleted or remodeled state in TME is indispensable for TNBC initiation and progression, and immunotherapies targeting active chemokines in TME are gradually being studied and recognized.<sup>4</sup>

Besides tumor cells, TME is a complex integrated system with a complicated population of non-tumor cells including immune cells and stromal cells, as well as non-cellular components such as extracellular matrix and cytokines. Among them, the signaling of chemokines and their chemotactic properties toward various cell populations play a central role in the composition of immunosuppressive TME.<sup>5</sup> C-C chemokine ligand 5 (CCL5) is highly expressed in TNBC and is seldom expressed constitutively in normal breast epithelial duct cells, suggesting an active role of CCL5 in the initiation and progression of TNBC.<sup>6,7</sup> Due to its activities in the immune environment, CCL5 can induce leukocyte directed movement. Of note, macrophages, as one of the most infiltrated immune cells, could also be recruited by CCL5, when they are present in TME called tumor-associated macrophages (TAM). The higher the immunosuppressive degree of TME is progressed, the higher the count of M2 macrophages with tumor-promoting activity and the lower the count of M1 macrophages with tumor-suppressing activity are expressed.<sup>8,9</sup> Meanwhile, some cytokines secreted by TAM may inversely induce their irritator to malignant phenotypes, like TGF- $\beta$  and IL-10, which can simultaneously promote the polarization of TAM to malignant phenotype by autocrine and impair the function of immune cells in TME by paracrine. These can further deepen the immunosuppressive degree of TME, in turn which also implies the weakening of the anti-tumor response and further malignant progression of the tumor. CCL5 just as the chemokine that would be upregulated in TME as a result, can aggregate more TAM to exacerbate the immunosuppressive degree of TME, forming a vicious cycle to breed immune escape.<sup>7,10</sup> Therefore, targeting CCL5 in TME may possibly provide a promising avenue for the precise immunotherapy of TNBC.

MicroRNA (miRNA) is a group of small non-coding RNA molecules that can inhibit gene expression by cutting off mRNA or inhibiting the translation process.<sup>11</sup> According to our previous review, miRNAs play a crucial role in the process of tumor immune escape through specifically binding with certain nucleotide sequence to regulate the activity of whole pathways, thus restoring normal immune surveillance.<sup>12</sup> After database prediction, miR-588 levels are downregulated in TNBC, and more importantly, it is shown to target the 3'UTR of CCL5. In some previous studies, miR-588 can be used as a prognostic marker in lung cancer, gastric cancer and glioma, which is considered to have a potential significance in gene therapy.<sup>13–15</sup> However, a major limitation of using miR-588 alone as a therapeutic tool is that free miR-588 would be rapidly degraded by nucleases as well as cause extensive genotoxicity, due to its binding way to target genes with inefficient delivery into cells and tissues of interest.<sup>16</sup> Therefore, effective and targeted delivery of miRNA-based drugs to the tumor site with exosomes, liposomes, viruses and artificial nanoparticles have been extensively explored, among which exosomes came into our sight for its superior features.

In this study, human mesenchymal stem cell secreted exosomes (MSC-Exos) were used as carriers to load miR-588 by electroporation, owing to their excellent biocompatibility with low immunogenicity, tumor homing property and long circulating half-life.<sup>17</sup> MSC-Exos loaded miR-588 can harness cell-to-cell communication within the TME, and might deliver cargoes across the physiological barriers within the body that often confine the penetration of other synthetic nanocarriers. To elevate specific delivery, engineered exosome strategy was applied to enhance the uptake of TNBC cells, through modifying  $\alpha$ (RGDyK) (referred to as cRGD) on the surface of exosomes. The highly expressed  $\alpha\beta 3$  integrin receptor on the surface of TNBC cells has a high affinity with cRGD, which may lead to better efficacy and reduced systemic toxicity of this delivery system.

Herein, we designed and prepared an engineered exosome with cRGD modification for effective delivery of miR-588 to TNBC, aiming to remodel immunosuppressive TME by anchoring CCL5. It also provided new insights into the treatment of TNBC to explore the potential of miRNA-based precise immunotherapy on TME combined with engineered exosomal carriers against TNBC (Figure 1).

## Methods

### Materials

MDA-MB-231 (human breast cancer cell line) and HEK-293 (human embryonic kidney cell line) were purchased from BNCC (Beijing, China). The two cell lines above were cultured in high-sugar Dulbecco's Modified Eagle Medium (DMEM,

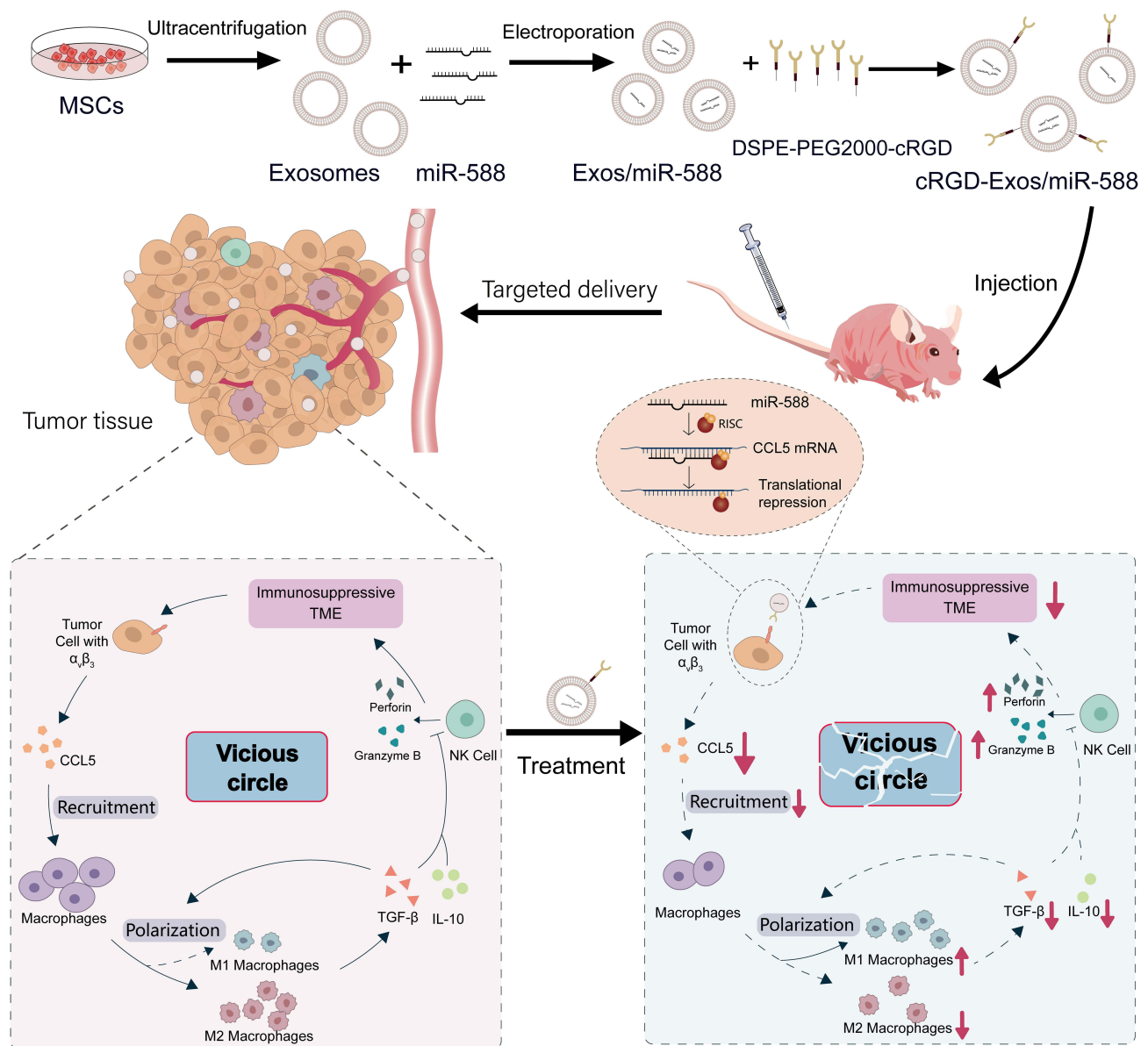


**Figure 1** Schematic illustration of the synthesis of cRGD-Exos/miR-588 and the mechanism of anti-tumor, remodeling effect on the immunosuppressive TME.

Biorigin, Beijing, China) supplemented with 10% fetal bovine serum (FBS; Corning, USA) and 1% penicillin (100 U/mL)/streptomycin (100 mg/mL) and maintained at 37 °C in 5% CO<sub>2</sub>. MSCs (hTERT immortalized adipose derived Mesenchymal stem cells, Hefei SynthBiological Engineering Co., Ltd, Anhui, China) were cultured in mesenchymal stem cell complete medium (Hefei SynthBiological Engineering Co., Ltd, Anhui, China). DSPE-PEG2000-c(RGDfk) were obtained from Xi'an ruixi Biological Technology Co., Ltd (Shaanxi, China) and PKH67 was from Sigma (USA). Bovine Serum Albumin (BSA) and 1.1-dioctadecyl-3,3,3,3-tetramethylindotricarbocyanine iodide (DiR) fluorescent probe was obtained from LABLEAD BIOTECHNOLOGY CO., LTD (Beijing, China). miR-588 mimic, miR-588 inhibitor and negative control were purchased from GenePharma (Shanghai, China). The sequences are as follows: miR-588 mimic, sense UUGGCCACAAU GGGUAGAAC, and antisense UCUAACCAUUGUGGCCAAUU; mimic negative control, sense UUCUCCGAAC GUGUCACGUTT, antisense ACGUGACACGUUCGAGAATT; miR-588 inhibitor, sense GUUCU AACCAUUG UGGCAA; inhibitor NC, sense CAGUACUUUUGUGUAGUACAA.

## RNA Isolation and Quantitative Real-Time PCR (qPCR)

FastPure<sup>®</sup> Cell/Tissue Total RNA Isolation Kit V2 (Vazyme, China) was used to extract RNA. Hairpin-it<sup>TM</sup> microRNA and U6 snRNA Normalization RT-PCR Quantitation Kit (GenePharma, China) was used for miRNA. For RNA, HiScript<sup>®</sup> III All-in-one RT SuperMix Perfect for qPCR (Vazyme Biotech, China) was used for reverse transcription and Taq Pro Universal SYBR qPCR Master Mix (Vazyme Biotech, China) was used for qPCR. Results were obtained using the CFX96<sup>TM</sup> Real-time System 3.1 software (Applied Bio-Rad). A minimum of 3 replicate wells were set up for each sample and further analyzed using the  $2^{-\Delta\Delta C_t}$  method with U6 as the internal reference gene. All primers used in qPCR were synthesized by Sangon Biotech Co., Ltd. (Shanghai, China). The primer sequences were as follows: miR-588, forward GATGCTCTTTGGCCACAATG, and reverse TATGGTTGTTCTGCTCTCTGTCTC; U6, forward CGCTTCGGCAGCACATATAC, and reverse TTCACGAATTTGCGTGTCTATC; CCL5, forward ATTTGCCTGTTTCTGCTTGCTCTTG, and reverse AACTGCTGCTGTGTGGTAGAATCTG; TGF- $\beta$ , forward AAGGTGAGGAAACAAGCCCAGAG, and reverse AAGTGCTAGGATTACAGGCGTGAG; GAPDH, forward AGATCCCTCCAAAATCAAGTGG, and reverse GGCAGAGATGATGACCCTTTT.

## Dual-Luciferase Reporter Gene Assay

The plasmids used in this experiment were purchased from Fenghui Bio. The wild-type plasmid psiCHECK2-CCL5-WT was formed by cloning the fragment containing the miR-588 binding site using the psiCHECK2 vector as the backbone, and the mutant plasmid psiCHECK2-CCL5-MUT containing the mutation site. Before transfection, MDA-MB-231 cells ( $1.2 \times 10^6$  cells/well) were inoculated in 6-well plates and then cotransfected with the corresponding miRNA mimic or negative control using Lipofectamine 3000 (Invitrogen, USA). 24 hours after transfection, the activities of the two luciferase enzymes were measured sequentially according to the instructions.

## Exosome Isolation and Purification

Exosomes were obtained from immortalized MSCs. MSCs were cultured in MSC complete medium and when cell density reached 60–70%, the medium was changed to MSC complete medium with exosomes removed FBS. Two days later, cell culture supernatant was collected and centrifuged in high-speed micro centrifuge (CF16RN, himac, Japan) at 300 g for 10 min to remove cells. The supernatant was centrifuged at 2,000 g for 10 min and 10,000 g for 30 min to remove dead cells and cell debris. The supernatant was taken and centrifuged twice at 120,000 g for 70 min each time in an ultracentrifuge (optima xpn-100, BECKMAN COULTER, USA) which had been pre-cooled to 4 °C. The final microspheres were resuspended in PBS and stored at –80 °C.

## Preparation of cRGD-Exos/miR-588

Loading miRNA into exosomes was performed by electroporation. Exosomes were mixed with miR-588 mimic at a ratio of 1:1. Dilution to 0.5 mg/mL in pre-cooled 0.4 mm tubes with electroporation buffer. Electroporation was performed on GenePulser (BioRad) programmed with 400 mV and 125  $\mu$ F capacitance (pulse time 10–15 ms) to obtain Exo/miR-588. The method of modifying cRGD onto exosomes was referred to the post-insertion method in previous studies,<sup>18</sup> which utilizes the property that DSPE-PEG molecules can be efficiently inserted into phospholipid bilayers. DSPE-PEG2000-cRGD was treated in 4-(2-hydroxyethyl)-1-piperazineethanesulfonic acid buffer (HEPES) to form micelles and then sonicated to reduce the micelle size and facilitate separation. The exosome suspension was mixed with micellar solution at 40 °C for 2 hours and immediately cooled to 4 °C. After centrifugation at 120,000 g for 70 min, the precipitate was resuspended with PBS to obtain cRGD-Exos/miR-588.

## Characterization of cRGD-Exos/miR-588

The morphology as well as the size distribution of Exos, Exos/miR-588, cRGD-Exos/miR-588 were characterized by transmission electron microscopy (TEM) and Nano-ZEN3600. The surface markers of exosomes were characterized using Western Blot. The antibodies were CD9 antibody (1:1000, Abcam), TSG-101 antibody (1:1000, Abcam), and Calnexin



antibody (1:1000, Abcam). The miR-588 content of Exos and Exos/miR-588 were measured separately by qPCR to demonstrate that miR-588 had been successfully loaded.

## In vitro Cellular Uptake Assays

After diluting the exosomes with Diluent C, an equal volume of PKH67 staining solution was added and the reaction was carried out for 2 min protected from light. 1% BSA was used to terminate the staining, and the exosomes were purified by centrifugation at 120,000g for 70 min and resuspended in PBS to obtain fluorescently labeled exosomes. PKH67-labeled Exos/miR-588 and cRGD-Exos/miR-588, respectively, were added to MDA-MB-231 cells. After co-culture for 12 hours, cellular uptake of cRGD-Exos/miR-588 was evaluated by detecting the average fluorescence intensity of cells using FACSCalibur flow cytometer (BD Biosciences, USA).

## Cell Viability Assay

cRGD-Exos/miR-588 was evaluated for cytotoxicity on MDA-MB-231 cells. Cells were seeded in 96-well plates ( $1 \times 10^4$  cells/well) one day in advance and then given different concentrations of free miR-588 and cRGD-Exos/miR-588. After one day, the medium was discarded and replaced with 90  $\mu$ L of fresh medium and 10  $\mu$ L of CCK-8 solution. After incubation at 37 °C for 3 hours, the absorbance at 450 nm was measured using an enzyme marker (Biotek Epoch, USA). Cell viability was calculated as follows.

$$\text{Cell viability (\%)} = \frac{OD_{\text{Sample}} - OD_{\text{Blank}}}{OD_{\text{Control}} - OD_{\text{Blank}}} \times 100\%$$

## Enzyme Linked Immunosorbent Assay (ELISA)

The levels of CCL5 and TGF- $\beta$  in vitro and the levels of Granzyme B, perforin, TGF- $\beta$  and IL-10 in vivo were detected by ELISA. Kits for CCL5 and Granzyme B were purchased from R&D Systems (CCL5, ELH-RANTES-1; Granzyme B, ELM-GranzymeB-1). Kits for perforin, TGF- $\beta$ , and IL-10 were purchased from ABclonal (Perforin, RK03133; IL-10, RK00016; TGF- $\beta$ , RK00055 and RK00057). Cell culture supernatants or tumor tissues were collected and assayed according to the manufacturer's instructions.

## Tumor-Bearing Nude Mouse Model

Six-week-old BALB/c female nude mice were purchased from Beijing Life River Experimental Animal Technology Co., Ltd. and kept in a sterile environment, fed for one week for acclimatization and familiarized with the environment before the experiment. Experimental protocols involving laboratory animals were approved by the Laboratory Animal Ethics Committee of Nanjing Ramda Pharmaceutical Co. Ltd (License No. IACUC-20230310) and conducted in accordance with the Guide for the Care and Use of Laboratory Animals. MDA-MB-231 cells ( $3 \times 10^6$ /mL, 200  $\mu$ L) were injected into the armpit of nude mice to establish a tumor model. Note the state of tumor generation in mice and measure the length (L) and width (W) of subcutaneous tumors, and calculate the tumor volume using the formula  $(L \times W^2)/2$ . The experiment was performed after the tumor volume reached 90 mm<sup>3</sup>.

## In vivo Distribution Assays

The successfully tumor-bearing mice were randomly divided into two groups and used to investigate the tumor-targeting potential of cRGD-Exos/miR-588 in vivo. cRGD-Exos/miR-588 was incubated with 5 mM of DiR fluorescent probe at 37°C for 15 min, and then centrifuged in ultracentrifuge pre-cooled to 4 °C at 120,000 g for 70 min to remove excess dye. The precipitate was resuspended with PBS to obtain DiR-labeled cRGD-Exos/miR-588. 200  $\mu$ L of cRGD-Exos/miR-588 were injected via tail vein at 1 mg/kg. The control group was injected with DiR. Fluorescence images were acquired at 1 h, 4 h, 8 h, 12 h and 24 h after injection using an in vivo fluorescence imaging system (Xenogen, Alameda, USA). DiR-labeling cRGD-Exos/miR-588 had an excitation wavelength of 748 nm and an emission wavelength of 780 nm.

## In vivo Anti-Tumor Effect

Mice bearing tumors were randomly divided into three groups: saline, free miR-588 and cRGD-Exos/miR-588. Each mouse was injected with the corresponding drug (200  $\mu$ L, 5 nmol,  $1 \times 10^{10}$  particles/each) via tail vein on days 0, 3, 6, 9 and 12, and the body weight of the mice was recorded in real time. After 14 days of treatment mice were sacrificed and tumors were collected, photographed and measured for volume and weight.

## Immunohistochemistry (IHC)

The expression levels of CCL5 in tumor tissue were determined by IHC. A portion of the tumor tissue was fixed using 4% paraformaldehyde fixation solution at 4 °C, dewaxed, and hydrated. After sufficient washing with PBS, add pre-warmed closure permeation solution. After closure with serum, incubate with CCL5 primary antibody (NO: 710,001; Thermo Fisher) at 4 °C overnight. Incubate with secondary antibody for one hour and stain with DAB and hematoxylin.

## Flow Cytometry Analysis of the Macrophage Counts

The number of macrophages in the tumor was determined by flow cytometry. Tumor tissue was ground and digested with 1 mg/mL of collagenase for 1 hour. Digested cells were filtered through cell filters and then separated by density gradient centrifugation. After obtaining single-cell suspensions, macrophages were extracted using Mouse Tumor Tissue Macrophage Isolation Solution Kit, according to the instructions guidelines. They were then incubated with different fluorescent dye-labeled monoclonal antibodies for 10 min at room temperature protected from light. They were then analyzed by flow cytometry and FlowJo software. Macrophages were identified as CD68<sup>+</sup>, M1 macrophages as CD206<sup>+</sup>, and M2 macrophages as CD86<sup>+</sup>.

## In vivo Safety Evaluation

To assess the safety of cRGD-Exos/miR-588, mice were sacrificed after drug administration and vital organs (heart, liver, spleen, lung and kidney) were collected. The organs were fixed and embedded in paraffin, cut into 5 mm sections, stained with conventional hematoxylin and eosin (H&E), and observed and recorded under the microscope.

## Statistical Analysis

All data are expressed as mean  $\pm$  standard deviation. Statistical analysis was performed using Prism graph pad 8.0. Paired or unpaired Student's *t*-test or ANOVA were used to compare between-group differences. Significance The level of significance was set at  $P < 0.05$ .

## Result

### CCL5 is the Target of miR-588

The public database TargetScan was used to predict miRNAs targeting CCL5. Among them, miR-588, which was confirmed to be abnormally low expressed in TNBC tissues, was focused on and subsequently verified (Figure 2A). To this end, we designed a dual luciferase plasmid for miR-588 and CCL5 (Figure 2B). The results of dual luciferase reporter assay further confirmed the targeting relationship between CCL5 and miR-588. The luciferase activity of miR-588 mimic and CCL5-3' UTR-WT transfected group was significantly lower than that of NC and CCL5-3' UTR-WT cotransfected group. In contrast, overexpression of miR-588 had no effect on luciferase activity in the mutant group (\*  $P < 0.05$ ; Figure 2C), suggesting that miR-588 targeted CCL5 via the 3' UTR. These results suggest that increased expression of CCL5 in the TME of TNBC correlates with aberrant expression of miR-588, meaning that changes in miR-588 expression can affect the expression level of CCL5.

### Preparation and Characterization of cRGD-Exos/miR-588

During the preparation of cRGD-Exos/miR-588, the step product was characterized by TEM, Western blotting and NTA. Western blotting analysis confirmed that all three groups of exosomes expressed the exosome markers CD9, TSG101, and did not express calnexin, and there was no significant difference among the three groups (Figure 3A). The results of NTA showed

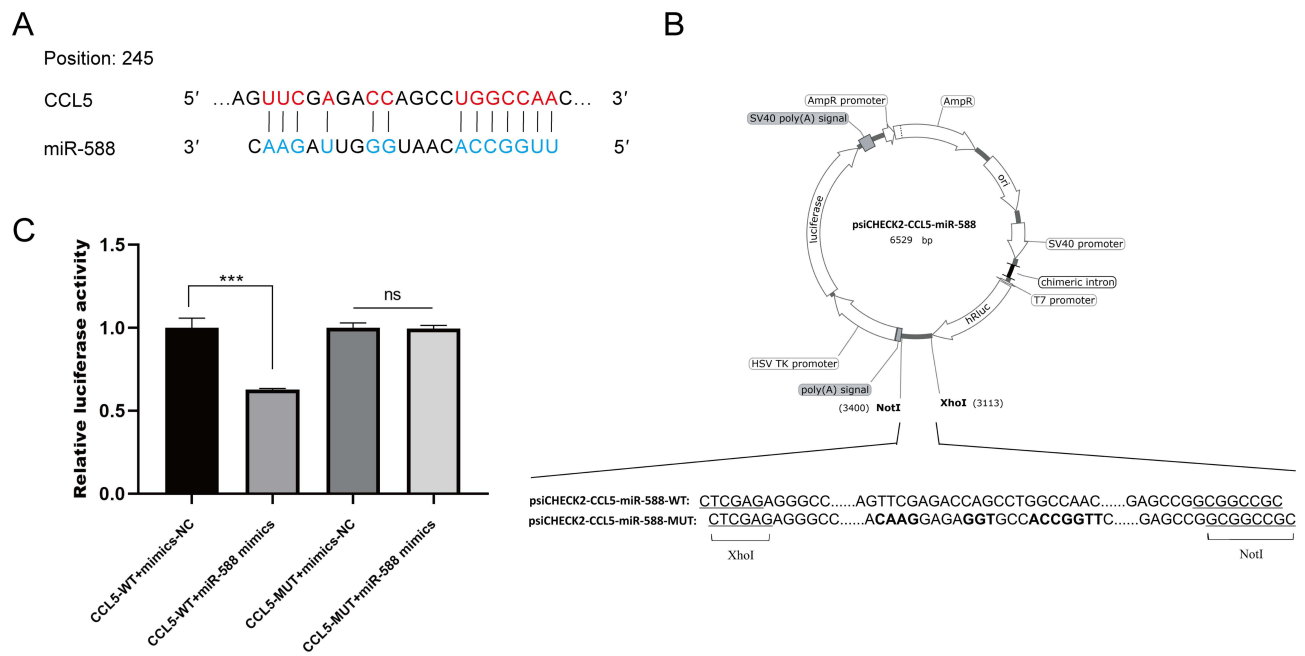


**Figure 2** (A) Predicted binding sites in the TargetScan public database. (B) Plasmids were designed and synthesized. (C) Relative luciferase activity of constructs containing wild-type or mutant CCL5 reporter genes in cells transfected with negative control or miR-588. Renilla luciferase was used as the reporter gene; firefly luciferase was used as an internal reference reporter gene for normalization. Statistics were represented as mean  $\pm$  SD. \*\*\* $P < 0.001$ .

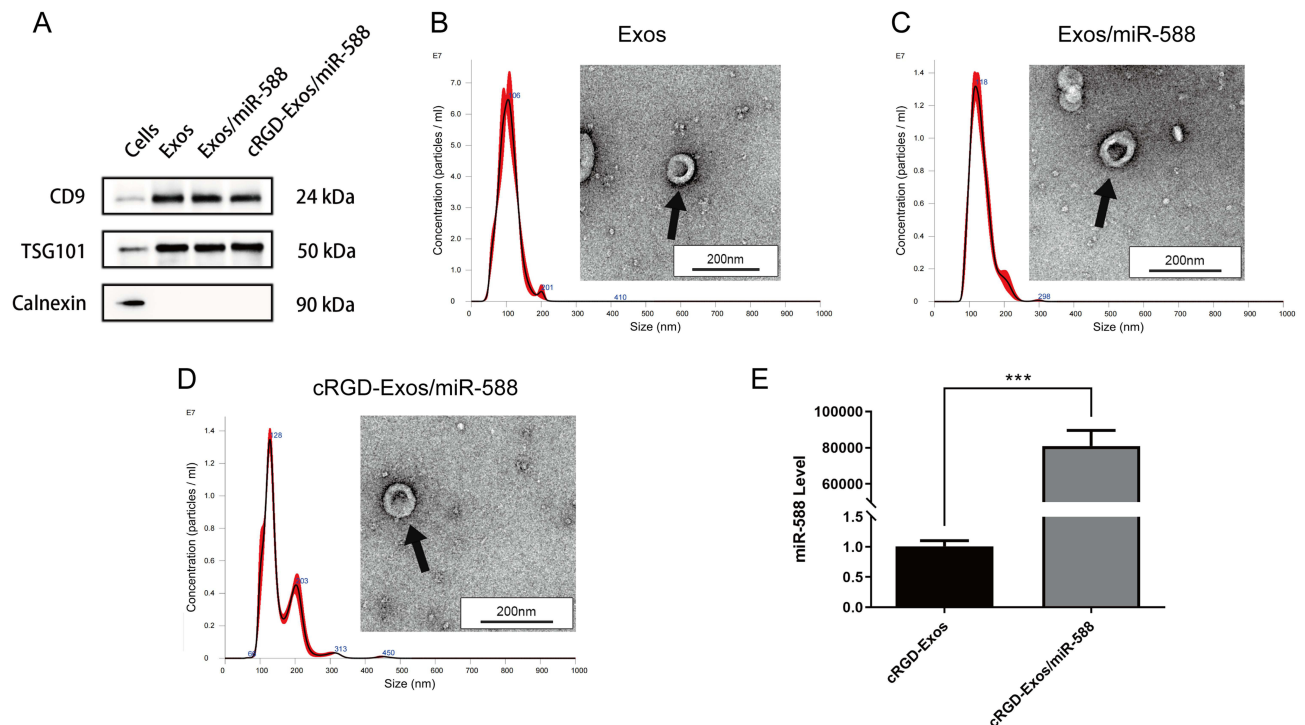


**Figure 3** Preparation and characterization of cRGD-Exos/miR-588. (A) Western blotting analysis of CD9, TSG-101, and Calnexin from MSCs, Exosomes, Exos/miR-588 and cRGD-Exos/miR-588. Representative TEM images and particle size distribution of (B) Exos, (C) Exos/miR-588 and (D) cRGD-Exos/miR-588 (scale bar = 200 nm). (E) qPCR result of miR-588 in Exos and Exos/miR-588. \*\*\* $P < 0.01$ .

that the mean particle sizes of Exos, Exos/miR-588, and cRGD-Exos/miR-588 all had physically uniform particle size distributions with mean particle sizes of  $106.1 \pm 28.4$  nm,  $133.0 \pm 30.1$  nm,  $153.8 \pm 50.1$  nm (Figure 3B–D). Meanwhile, Exos, Exos/miR-588, and cRGD-Exos/miR-588 all showed a typical disc-like bilayer structure (Figure 3B–D). Furthermore, to confirm that miR-588 was successfully loaded into the exosomes, qPCR was used to detect the miR-588 content before and after electroporation. The results are shown in Figure 3E, cRGD-Exos/miR-588 showed a significant increase in miR-588 content compared to cRGD-Exos, indicating that miR-588 mimics were successfully loaded into the exosomes by electroporation. All the above results demonstrate that cRGD-Exos/miR-588 was successfully prepared and the exosomes maintained structural integrity before and after modification and loading.

## In vitro Cellular Uptake of cRGD-Exos/miR-588

To evaluate the in vitro tumor-targeting ability of cRGD-Exos/miR-588 and assess whether cRGD modification could enhance the binding ability of exosomes to MDA-MB-231 cells, we used PKH67 labeled Exos/miR-588 and cRGD-Exos/miR-588 and co-cultured them with MDA-MB-231. After 6 h of incubation, cell uptake efficiency was determined by flow cytometry to measure the fluorescence intensity of MDA-MB-231 cells with PKH67-labeled Exos/miR-588 and cRGD-Exos/miR-588. The results showed that the cRGD-Exos/miR-588 group possessed stronger fluorescence intensity, which means a higher cellular uptake rate (Figure 4A and B). These results suggest that cRGD-Exos/miR-588 has a strong tendency to target tumors in vitro and that the cRGD could enhance the binding ability of exosomes to MDA-MB-231 cells.

## Cytotoxicity of cRGD-Exos/miR-588 in vitro

CCK-8 experiments were used to investigate the cytotoxicity of different concentrations of cRGD-Exos/miR-588 and free miR-588 on TNBC cells and normal cells. As shown in the Figure 5A, HEK-293 cells given free miR-588 showed a decrease in cell viability, while the cell survival rate of HEK-293 cells in the cRGD-Exos/miR-588 group was not significantly different from that of the control group. Meanwhile, the proliferation of TNBC cells treated with the two different drugs appeared to be inhibited (Figure 5B). In addition to  $IC_{50}$  in Figure 5C, selectivity index (SI) was employed as an indicator to assess anticancer activity. The SI of free miR-588 was 0.86, and the SI of cRGD-Exos/miR-588 was 11.72. When  $SI \geq 10$  was considered selective and can be further studied. This suggests that cRGD-Exos/miR-588 has anticancer activity with good selectivity. miRNAs have a wide range of mechanisms of action, and if they are to be administered in vivo as a therapeutic tool, a targeted vector must be available to deliver them to the specified location.

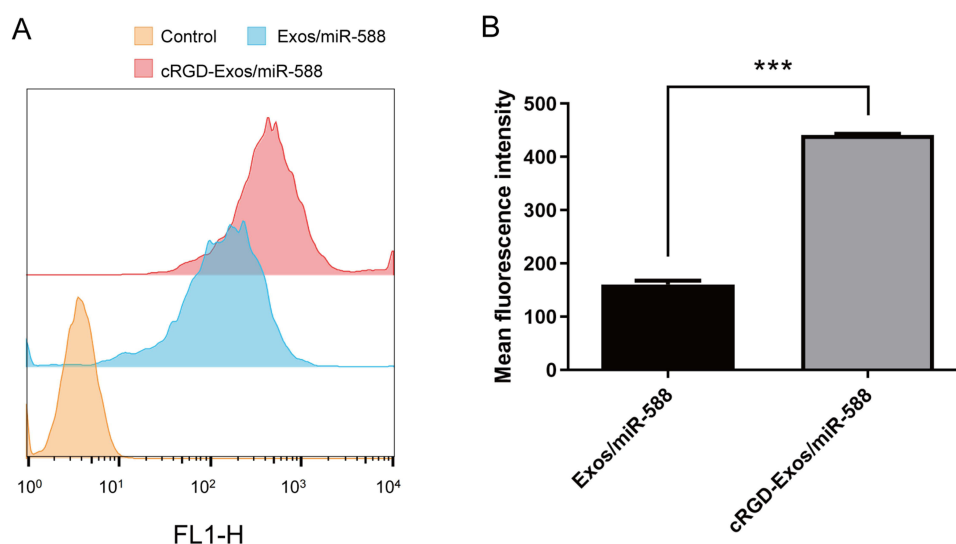


**Figure 4** (A) Flow cytometry analysis of MDA-MB-231 cells after incubation with PBS, Exos/miR-588, cRGD-Exos/miR-588. Exosomes were stained with PKH67. (B) Quantitative mean fluorescence intensity analysis of PKH67-labeled Exos/miR-588 and cRGD-Exos/miR-588 binding to MDA-MB-231 cells. Statistics were represented as mean  $\pm$  SD. \*\*\* $p < 0.001$ .

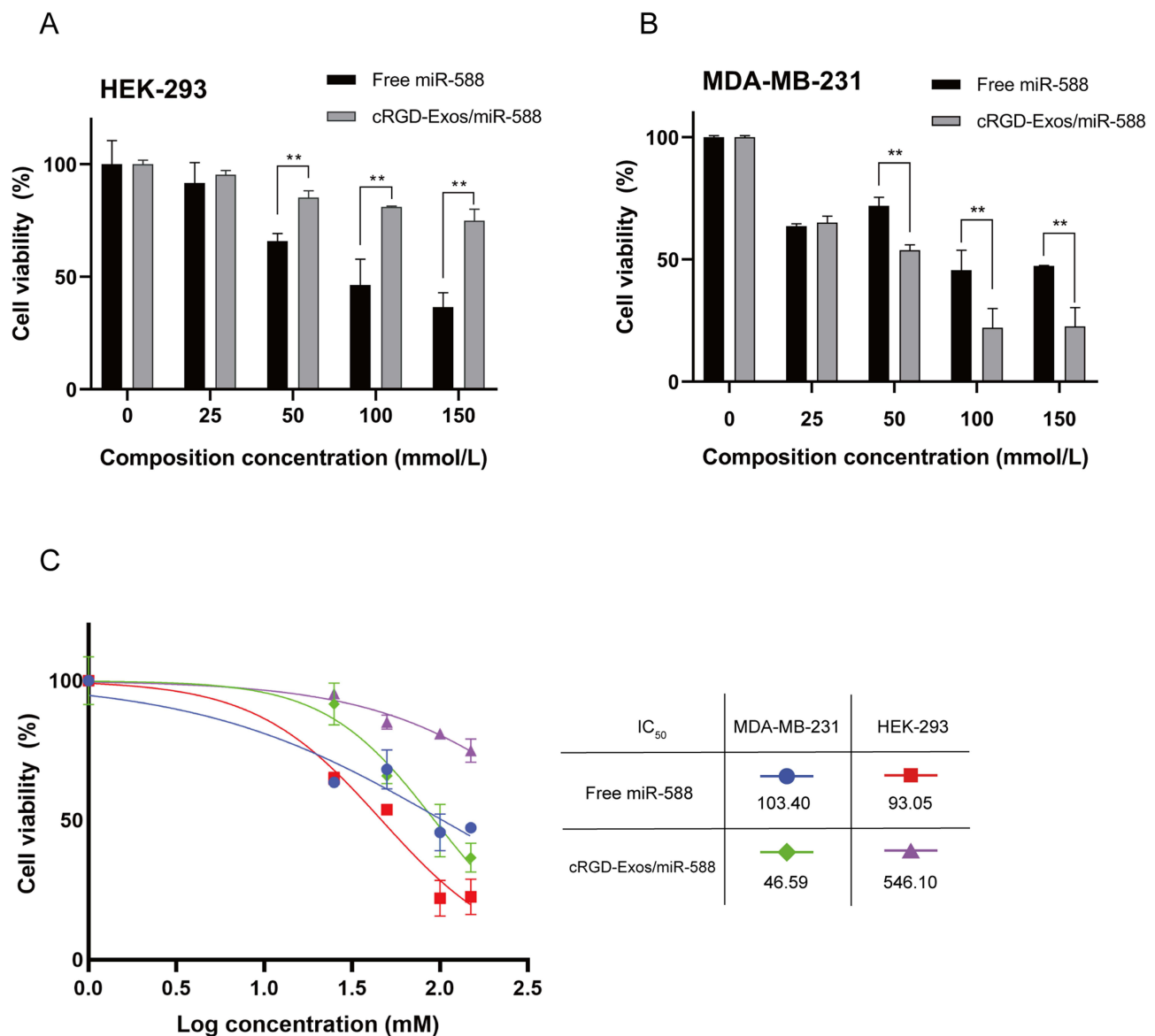


**Figure 5** In vitro cytotoxicity of free miR-588 and cRGD-Exos/miR-588 on (A) HEK-293 cells. (B) MDA-MB-231 cells. (C) IC<sub>50</sub> of free miR-588 and cRGD-Exos/miR-588 in MDA-MB-231 and HEK-293. In all graphs, statistics were represented as mean  $\pm$  SD. \*\* $P < 0.01$ .

And miRNAs have a wide range of mechanisms of action and require targeted carriers to deliver them to the designated sites for therapeutic effects.

## The Effects of cRGD-Exos/miR-588 in vitro

Next, we examined the effect of cRGD-Exos/miR-588 on TNBC cells. MDA-MB-231 cells were co-incubated with free miR-588 and cRGD-Exos/miR-588 for 48 hours, cell supernatants were collected as well as RNA was extracted to assess the level of miR-588 in order to confirm whether cRGD-Exos/miR-588 could effectively deliver miR-588. The results showed that the content of miR-588 was significantly increased after treatment with cRGD-Exos/miR-588 (Figure 6A). TGF- $\beta$ , as an immunosuppressive factor, has a pro-tumorigenic effect by regulating genomic instability, immune evasion and metastasis, and can be used as a marker for immunosuppressive TME.<sup>19,20</sup> It could induce macrophage polarization to M2 through paracrine as well as autocrine, which further aggravates the degree of immunosuppression of TAM.<sup>21</sup> In addition, TGF- $\beta$  is a powerful inhibitor of NK cells that can inhibit NK cells cytotoxicity.<sup>22</sup> The transcriptional levels of CCL5 and TGF- $\beta$  were detected by qPCR, and the results showed that CCL5 and TGF- $\beta$  declined after treatment (Figure 6B and C). Among them,



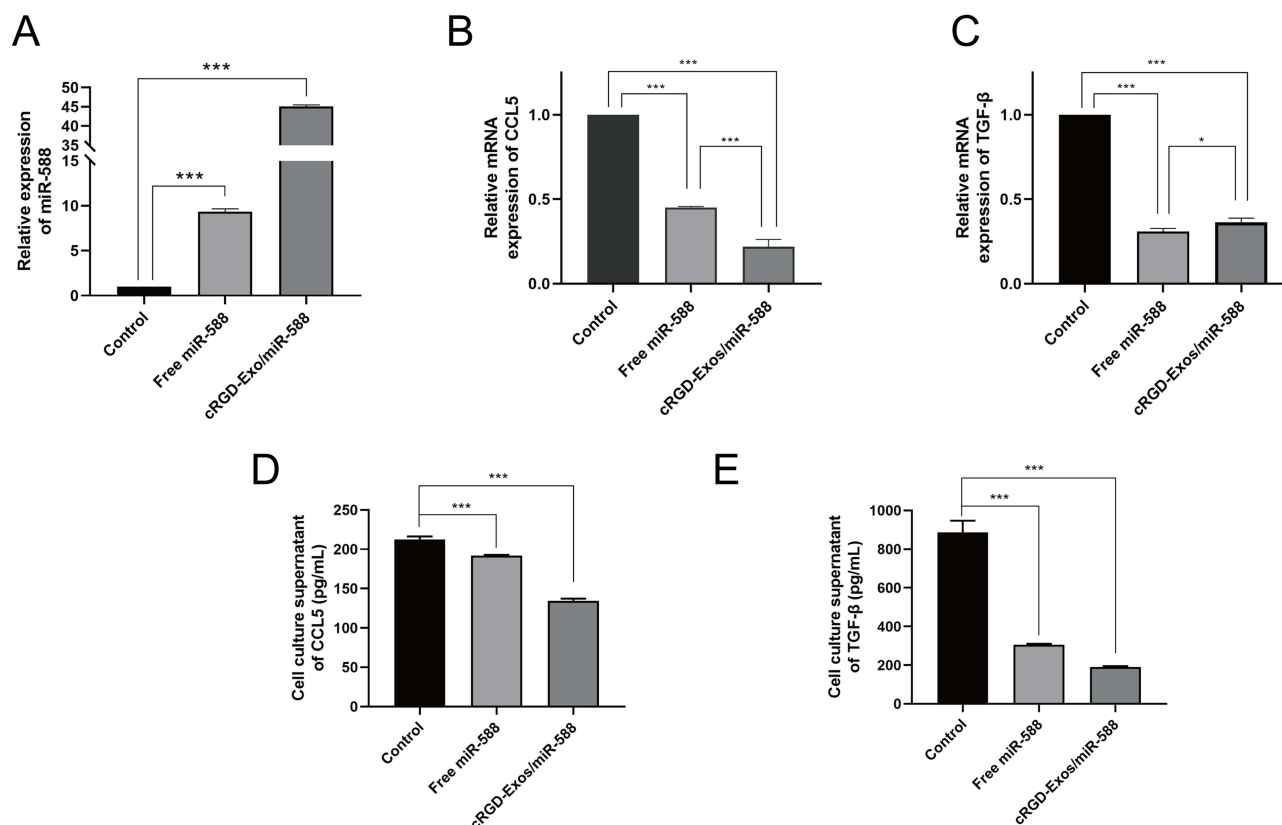


**Figure 6** Effect of cRGD-Exos/miR-588 on miR-588, CCL5 and TGF-β. (A–C) qPCR results of miR-588, CCL5 and TGF-β. The ELISA results of CCL5 (D) and TGF-β (E). In all graphs, statistics were represented as mean ± SD. \* $p < 0.05$ , \*\*\* $p < 0.001$ .

for TGF-β was slightly higher in the free miR-588 group than in the engineered exosome group, probably because the exosomes may contain TGF-β or components that lead to its increased level. Since both CCL5 and TGF-β are cytokines, ELISA assay was used to determine their protein levels. The results showed that two cytokines were significantly reduced after cRGD-Exos/miR-588 treatment (Figure 6D and E). Taken together, these studies suggest that cRGD-Exos/miR-588 can effectively deliver miR-588 into cells, thereby affecting the expression of CCL5 and TGF-β.

### Anti-Tumor Effect of cRGD-Exos/miR-588 in vivo

To further confirm the anti-tumor effect of cRGD-Exos/miR-588 in vivo, we tested the therapeutic efficacy in tumor-bearing nude mice. We firstly evaluated the effect of different therapeutic substances on tumor growth. Compared with the control group, tumor growth was inhibited after free miR-588 and cRGD-Exos/miR-588 treatments (55.37% tumor inhibition in the free miR-588 group and 80.15% tumor inhibition in the cRGD-Exos/miR-588 group; Figure 7A and B). The results showed that free miR-588 by tail vein injection had some inhibitory effect on TNBC tumors, but the inhibitory effect was more obvious in the cRGD-Exos/miR-588 group. This confirms the anti-tumor efficacy of cRGD-Exos/miR-588 and the importance of tumor targeting ability for effective treatment of TNBC.

### Remodeling Effect of cRGD-Exos/miR-588 on the Immunosuppressive TME

Next, to further evaluate the remodeling effect of cRGD-Exos/miR-588 on the immunosuppressive TME, we evaluated CCL5, the count of macrophages in tumor tissues and multiple cytokines assays. The first was the expression of CCL5, which was significantly reduced after cRGD-Exos/miR-588 treatment. In contrast, free miR-588 treatment resulted in less change of CCL5 expression, indicating that miR-588 alone was unable to fully exert its effects in vivo (Figure 8A). Subsequently, flow cytometry results showed a decrease in the count of tumor-promoting M2 macrophages and an increase in the count of tumor-suppressing M1 macrophages of the cRGD-Exos/miR-588 group (Figure 8B), implying

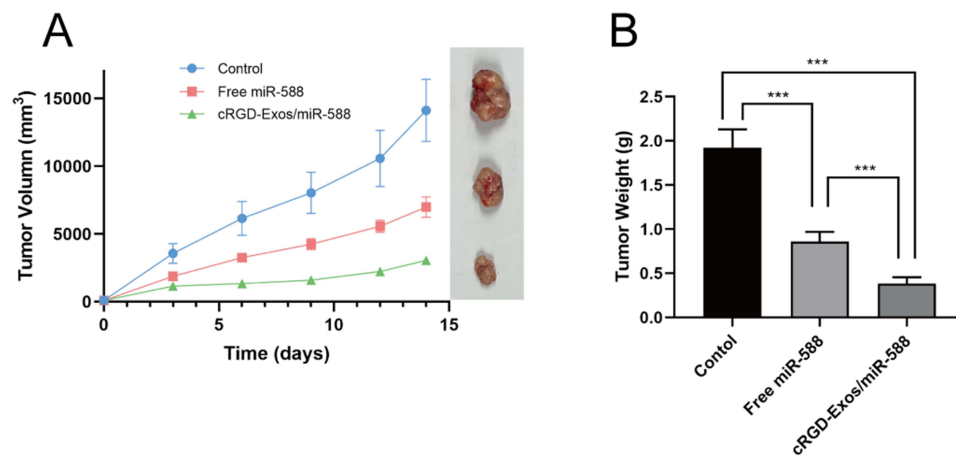


**Figure 7** Anti-tumor effect in vivo. Tumor volume (A) and tumor weight (B) of BALB/c nude mice in each group after treatment. \*\*\* $P < 0.001$ .

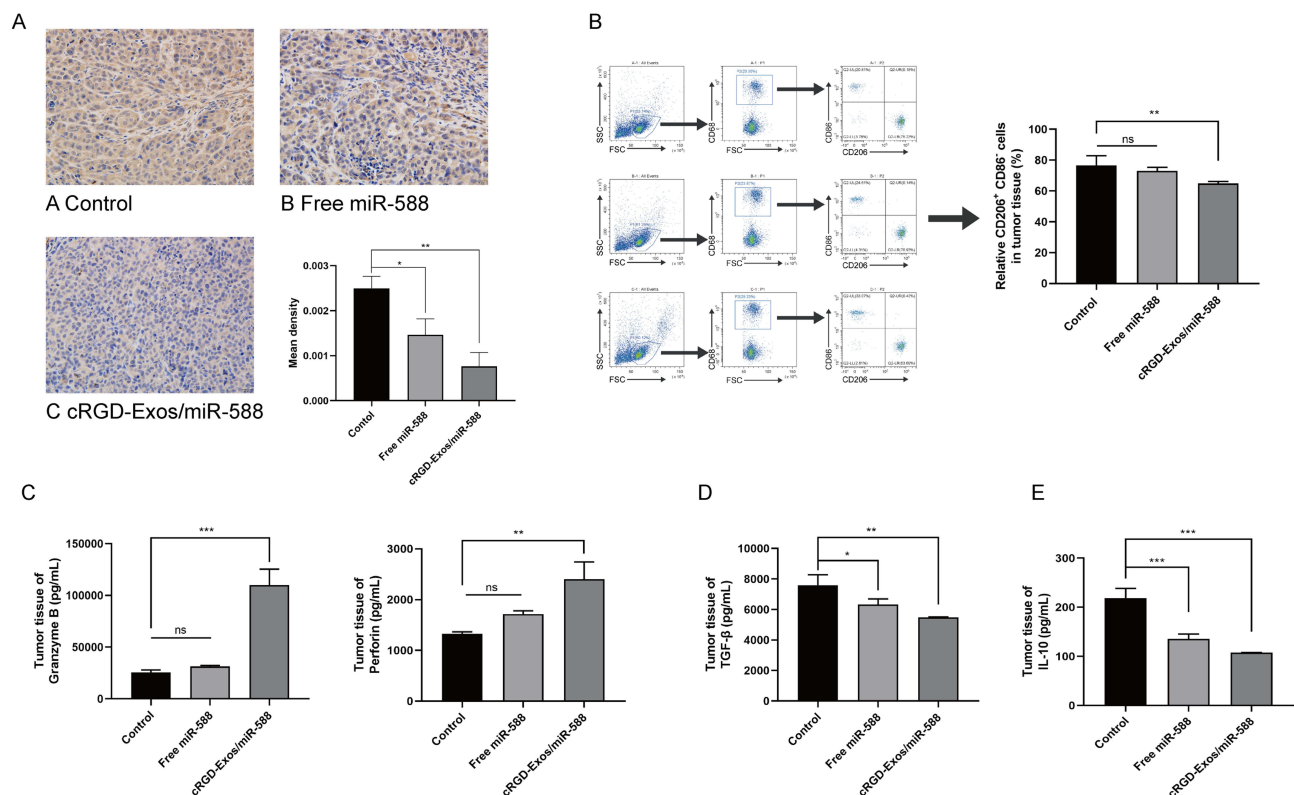


**Figure 8** Remodeling effect on immunosuppressive TME. (A) Representative IHC images of CCL5 in tumor tissues (original magnification = $\times 400$ ). (B) Representative flow cytometry plots and statistical quantification of M2 macrophages (CD68<sup>+</sup>CD86<sup>+</sup>CD206<sup>+</sup> cells) in tumor tissues. (C) Levels of two killing mediators Granzyme B and Perforin of NK cells in tumor tissues. (D) Levels of IL-10 in tumor tissues. (E) Levels of TGF- $\beta$  in tumor tissues. \* $P < 0.05$ , \*\* $P < 0.01$ , \*\*\* $P < 0.001$ .

that treatment with cRGD-Exos/miR-588 produced antitumor effects by altering the polarization direction of TAM in tumor tissue. In addition, we also evaluated the cytotoxicity of NK cells by detecting the levels of killing mediator levels. The results showed that both granzyme B and perforin were significantly raised in the cRGD-Exos/miR-588 group compared with other controls (Figure 8C). Finally, cRGD-Exos/miR-588 also alleviated the immunosuppressive TME of TNBC. We assessed the levels of TGF- $\beta$  and IL-10 in tumor tissues, as these cytokines can be used as markers to assess the degree of immunosuppression in TME.<sup>23,24</sup> ELISA results showed that TGF- $\beta$  and IL-10 were significantly reduced in tumor after treatment with cRGD-Exos/miR-588 compared to the control group (Figure 8D and E), suggesting that that

the degree of immunosuppression of TME was reduced after treatment with cRGD-Exos/miR-588. These results indicated that cRGD-Exos/miR-588 can remodel TME by regulating CCL5 to adjust the polarization type of TAM, while enhancing the killing ability of NK cells, resulting in a reduced degree of immunosuppression and thus reaching anti-tumor efficacy.

## In vivo Tumor Targeting and Biodistribution Study

Given that cRGD-Exos/miR-588 exhibited good cellular uptake and targeting in vitro, we labeled cRGD-Exos/miR-588 with DiR and injected it via tail vein. The results of real-time imaging system showed that fluorescent signals were already present at the tumor 1 hour after injection, indicating that cRGD-Exos/miR-588 could rapidly target tumor for action. The fluorescent signal was highly expressed at tumor, but also appeared in the liver and spleen, which is consistent with the report that exosomes are most widely distributed in the liver and spleen.<sup>25</sup> The fluorescent signals in the liver and spleen almost disappeared 8 hours after injection, indicating that the engineered exosomes had been metabolized while exhibiting a strong fluorescence signal at the tumor site (Figure 9). These results suggest that cRGD-Exos/miR-588 can accumulate more effectively at tumor sites, perform well in targeted miRNA delivery of TNBC, and can be used as an effective delivery vehicle for targeting TNBC.

## In vivo Safety Evaluation

Apart from efficacy, toxicity is another key metric for evaluating a therapy. To this end, we measured body weight every day during treatment and sacrificed the mice at the end of treatment for H&E staining of important organs. During treatment, no mortality and severe weight loss were observed in the cRGD-Exos/miR-588 group (Figure 10A). H&E staining showed no significant damage to important organs in the cRGD-Exos/miR-588 group compared with the control group, and there was no obvious toxic and side effects, indicating that the engineered exosome delivery strategy has good in vivo safety (Figure 10B).

## Discussion

TNBC is the most aggressive and least prognostic subtype of breast cancer. Unlike other subtypes, the unique immunosuppressive TME is central to the ability of TNBC to avoid detection and elimination by the immune system. CCL5, as a molecular signal at the tumor site, plays a key role in recruiting immune cell infiltration and regulating inflammatory factors expression, which generates a suppressive environment to support tumor immune escape, making gene therapy targeting CCL5 a promising field. miRNAs, as genomic components, have been shown to potentially serve as a preferred pathway for immune escape in tumor cells. miR-588 is significantly associated with tumor progression, whose expression is reduced in TNBC cells, and more importantly, it is verified to target the 3'UTR of CCL5 by database prediction as well as by dual luciferase reporter assays for specifically blocking its expression. Correcting oncogenic

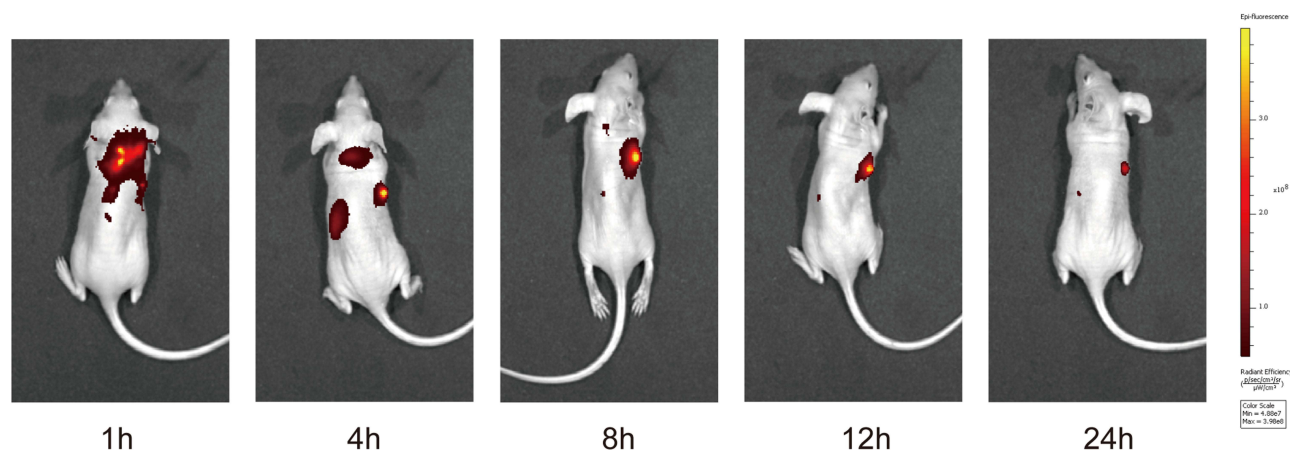


**Figure 9** In vivo tumor targeting studies. Fluorescence imaging at 1, 4, 8, 12, and 24 hours after cRGD-Exos/miR-588 injection.

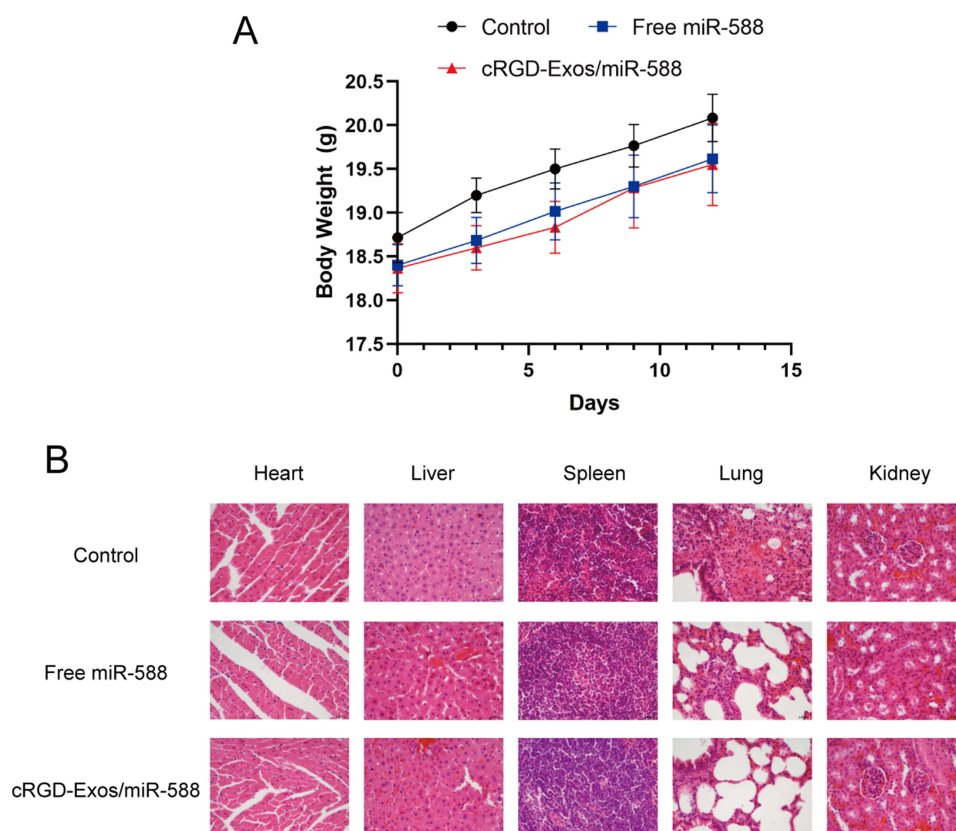


**Figure 10** In vivo safety evaluation. (A) Body weight of BALB/c nude mice in each group. (B) The representative results of H&E staining of important organs of BALB/c mice in each group. HE stained tissue sections were imaged at a magnification of 400 $\times$ .

alterations in gene expression through miR-588 anchored CCL5 in tumor cells that is responsible for the immunosuppressive microenvironment may be a powerful gene therapy for remodeling TME. However, miRNAs cannot be used as therapeutic tools alone to exert anti-tumor effects due to their own drawbacks such as universal genotoxicity, low bioavailability and off-target. Compared to liposomes and artificial nanoparticles, exosomes create opportunities for miRNA-based therapies with their excellent biocompatibility and the ability to act as natural carriers for intercellular macromolecular cargo and information exchange during physiological processes.<sup>26,27</sup> In this experiment, cRGD-modified exosomes were used as vehicles to carry miR-588 mimics for the targeted immunological treatment of TNBC by remodeling TME.

There are several challenges to be overcome in the development of engineered exosomes such as the efficient loading of miRNAs and their targeted delivery. Electroporation, as the earliest and most widely used method, has been applied to load miRNA, siRNA and some small molecule drugs. The characterization results showed that the morphology of cRGD-Exos/miR-588 still maintained the classic “cup-shape” structure of exosomes and the characteristic proteins on the membrane surface. The average particle size was  $153.8 \pm 50.1$  nm, which is in line with the general particle size of exosomes, and still possesses excellent biological properties such as stability, high efficiency and EPR effect. In addition, integrin receptor  $\alpha\beta3$ , which can interact with cRGD receptor ligands, is highly expressed in TNBC cells. Therefore, we modified the engineered exosomes with cRGD, so that they can selectively bind to  $\alpha\beta3$  through cRGD, and promote the interaction between engineered exosomes and tumor cells to achieve precise targeting of TNBC.<sup>28,29</sup> In this work, the subcutaneous xenograft tumor nude mouse model was used for the in vivo study. Although it was not possible to grow the tumor at the primary site as in the orthotopic xenograft tumor model, we chose to inject the tumor cells into the axilla, which is close to the mammary gland and has a rich distribution of lymphatic vessels. In this way, the reproducibility and success rate of modeling can be improved while better simulating the disease. One hurdle that must be overcome on the road to popularization of miRNA therapeutics is safety, so as to solve the problems of early degradation and genotoxicity. In in vivo safety experiments, the



obtained cRGD-Exos/miR-588 showed a better tumor targeting effect on MDA-MB-231 cells, and exhibited high enrichment at tumor sites after 24 hours. As for safety, cRGD-Exos/miR-588 was effective in reducing tumor weight while maintaining body weight in mice compared to free miR-588 treatment. Considering the excellent biological properties of exosomes exhibit good biocompatibility, circulating stability and size available for enhanced permeability and retention effects, furtherly, the targeted delivery function of engineered exosomes reduces the general genotoxicity caused by miRNA alone.

In TNBC, immunosuppressive TME is associated with abnormal low expression of miR-588, which is unable to constrain CCL5 expression, irritating a “vicious circle” at the site of tumor formation. IHC results showed that engineered exosomes could effectively reduce the expression of CCL5, relying on the effect of miR-588. CCL5 is identified as a key node of bidirectional communication between TNBC cells and normal cells, who can recruit TAMs from the circulation to tumor sites. This is due to its activity as a chemokine in the immune environment allowing it to induce directed migration of immune cells. In TNBC, abnormally elevated CCL5 results in a tendency for TAMs recruited to the tumor site under the influence of immunosuppressive TME to polarize into M2 macrophages with pro-tumorigenic activity rather than M1 macrophages with anti-tumorigenic activity. We observed that cRGD-Exos/miR-588 caused significant dynamic changes in macrophage subsets in TME, with a decrease in M2 macrophages and an increase in M1 macrophages by regulating CCL5 expression. In contrast, inflammatory factors such as TGF- $\beta$  and IL-10, which are secreted by TAMs and exacerbate the immunosuppressive degree of TME, were both downregulated after treatment. Because these inflammatory factors are thought to regulate the polarization process of TAMs to M2 macrophages through autocrine positive feedback. In addition, they can also act as inhibitors for the killing function of other infiltrating immune cells in TME through paracrine secretion on the other side. NK cells can kill tumor cells non-specifically and directly, without antigen sensitization or antibody involvement and MHC restriction, making them one of the main effector cells for killing tumor cells in TME. Despite their activity in controlling tumor growth, NK cells are sensitive to multiple immunosuppressive mechanisms activated in TME, including TGF- $\beta$  and IL-10 secreted by TAMs. These pleiotropic cytokines are known to down-regulate multiple aspects of NK cell function including cytokine secretion, degranulation and others. The results showed that cRGD-Exos/miR-588 was very effective in restoring cytotoxicity of NK cells inhibited by TGF- $\beta$  and IL-10, and re-establishing anti-tumor immune response. After a series of malignant phenotypes and inflammatory factors were suppressed while NK cells function was restored by these engineered exosomes delivered miR-588, the expression of the oncogenic mutation CCL5 in tumor cells was inhibited and the vicious cycle was cut off. Taken together, these studies support that cRGD-Exos/miR-588 can precisely transmit miR-588 into TNBC cells to remodel the immunosuppressive TME via anchoring CCL5, specifically inhibiting tumor malignant progression.

Although immunotherapy has shown exciting results in basic research and has made its way into clinical treatment, the benefits are limited in most cases due to the complexity of immune escape and the uncertainty of TME. Recently, it has been suggested that chemotherapy may affect the *in situ* immune conditions and cause a chain reaction, thereby increasing the response rate and efficacy of immunotherapy.<sup>30,31</sup> Given that monotherapy does not meet actual treatment needs, the combination of chemotherapy and immunotherapy for the treatment of TNBC has been used in the clinic and has shown promising efficacy.<sup>32</sup> However, there are still many clinical problems that need to be solved. It is believed that with the deepening research on tumor and TME mechanisms, immunotherapy combined with chemotherapy may become the mainstream treatment in the future.

## Conclusion

Taken together, the engineered exosomes modified with cRGD as a vehicle for miR-588 take full advantage of the property that exosomes can transport miRNAs shuttling between cells during biogenesis, which, together with the targeting ability of cRGD, may satisfy the need for a targeted as well as efficient delivery system for miRNAs. The cRGD-Exos/miR-588 can potentially anchor CCL5, thereby remodeling the immunosuppressive TME through affecting the expression of various cytokines in TME and the function of immune cells, thus restoring TAM polarization and infiltration. Immunotherapeutic strategies targeting TME have been recognized as very promising therapeutic strategies for the treatment of refractory tumors, but the interaction mechanisms of TME in the immunotherapeutic process are still not well defined. Current and future studies will explore the immunological characteristics and related mechanisms of TME in TNBC in greater depth and seek therapeutic modalities in combination with chemotherapy to provide the next generation of personalized immunotherapy of TNBC targeting its TME.



## Acknowledgments

This work was supported by The National Natural Science Foundation of China (82074269) Youth Qihuang Scholar of National Administration of Traditional Chinese Medicine (2020). A special thanks for the long-term subsidy mechanism from the Ministry of Finance and the Ministry of Education of PRC (People's Republic of China) for Beijing University of Chinese Medicine and China Academy of Chinese Medical Sciences.

## Disclosure

The authors declare that they have no competing interests or other interests that might be perceived to influence the results and discussion reported in this paper.

## References

1. Sung H, Ferlay J, Siegel RL, et al. Global cancer statistics 2020: GLOBOCAN estimates of incidence and mortality worldwide for 36 cancers in 185 countries. *CA Cancer J Clin.* 2021;71:209–249. doi:10.3322/caac.21660
2. Bou Zerdan M, Ghorayeb T, Saliba F, et al. Triple negative breast cancer: updates on classification and treatment in 2021. *Cancers.* 2022;14(5):1253. doi:10.3390/cancers14051253
3. Li Y, Zhang H, Merkher Y, et al. Recent advances in therapeutic strategies for triple-negative breast cancer. *J Hematol Oncol.* 2022;15(1):121. doi:10.1186/s13045-022-01341-0
4. Bhattacharya S, Khanam J, Sarkar P, Pal TK. A chemotherapeutic approach targeting the acidic tumor microenvironment: combination of a proton pump inhibitor and paclitaxel for statistically optimized nanotherapeutics. *RSC Adv.* 2019;9(1):240–254. doi:10.1039/c8ra08924h
5. Korbecki J, Grochans S, Gutowska I, Barczak K, Baranowska-Bosiacka I. CC chemokines in a tumor: a review of pro-cancer and anti-cancer properties of receptors CCR5, CCR6, CCR7, CCR8, CCR9, and CCR10 ligands. *Int J Mol Sci.* 2020;21:7619. doi:10.3390/ijms21207619
6. Aldinucci D, Borghese C, Casagrande N. The CCL5/CCR5 axis in cancer progression. *Cancers.* 2020;12(7):1765. doi:10.3390/cancers12071765
7. Velasco-Velázquez M, Xolalpa W, Pestell RG. The potential to target CCL5/CCR5 in breast cancer. *Expert Opin Ther Targets.* 2014;18(11):1265–1275. doi:10.1517/14728222.2014.949238
8. Mehla K, Singh PK. Metabolic regulation of macrophage polarization in cancer. *Trends in Cancer.* 2019;5(12):822–834. doi:10.1016/j.trecan.2019.10.007
9. Mehta AK, Kadel S, Townsend MG, Oliwa M, Guerriero JL. Macrophage biology and mechanisms of immune suppression in breast cancer. *Front Immunol.* 2021;12:643771. doi:10.3389/fimmu.2021.643771
10. Yu-Ju Wu C, Chen C-H, Lin C-Y, et al. CCL5 of glioma-associated microglia/macrophages regulates glioma migration and invasion via calcium-dependent matrix metalloproteinase 2. *Neuro Oncol.* 2020;22:253–266. doi:10.1093/neuonc/noz189
11. Meng L, Liu C, Lü J, et al. Small RNA zippers lock miRNA molecules and block miRNA function in mammalian cells. *Nat Commun.* 2017;8(1):13964. doi:10.1038/ncomms13964
12. Zhang Z, Huang Q, Yu L, et al. The Role of miRNA in tumor immune escape and miRNA-based therapeutic strategies. *Front Immunol.* 2021;12:807895. doi:10.3389/fimmu.2021.807895
13. Chen Y, Zhang J, Gong W, Dai W, Xu X, Xu S. miR-588 is a prognostic marker in gastric cancer. *Aging.* 2020;13(2):2101–2117. doi:10.18632/aging.202212
14. Yu M, Zhang X, Li H, Zhang P, Dong W. MicroRNA-588 is downregulated and may have prognostic and functional roles in human breast cancer. *Med Sci Monit.* 2017;23:5690–5696. doi:10.12659/msm.905126
15. Zhou X, Xu M, Guo Y, et al. MicroRNA-588 regulates invasion, migration and epithelial-mesenchymal transition via targeting EIF5A2 pathway in gastric cancer. *Cancer Manag Res.* 2018;10:5187–5197. doi:10.2147/CMAR.S176954
16. Chen L, Heikkinen L, Wang C, Yang Y, Sun H, Wong G. Trends in the development of miRNA bioinformatics tools. *Brief Bioinform.* 2019;20(5):1836–1852. doi:10.1093/bib/bby054
17. He C, Zheng S, Luo Y, Wang B. Exosome theranostics: biology and translational medicine. *Theranostics.* 2018;8(1):237–255. doi:10.7150/thno.21945
18. Zhu Q, Ling X, Yang Y, et al. Embryonic stem cells-derived exosomes endowed with targeting properties as chemotherapeutics delivery vehicles for glioblastoma therapy. *Adv Sci.* 2019;6:1801899. doi:10.1002/adv.201801899
19. Maruyama T, Chen W, Shibata H. TGF- $\beta$  and Cancer Immunotherapy. *Biol Pharm Bull.* 2022;45(2):155–161. doi:10.1248/bpb.b21-00966
20. Battle E, Massagué J. Transforming growth factor- $\beta$  signaling in immunity and cancer. *Immunity.* 2019;50(4):924–940. doi:10.1016/j.immuni.2019.03.024
21. Gratchev A. TGF- $\beta$  signalling in tumour associated macrophages. *Immunobiology.* 2017;222(1):75–81. doi:10.1016/j.imbio.2015.11.016
22. Viel S, Marçais A, Guimaraes FS-F, et al. TGF- $\beta$  inhibits the activation and functions of NK cells by repressing the mTOR pathway. *Sci Signal.* 2016;9(415):ra19. doi:10.1126/scisignal.aad1884
23. Dai E, Zhu Z, Wahed S, Qu Z, Storkus WJ, Guo ZS. Epigenetic modulation of antitumor immunity for improved cancer immunotherapy. *Mol Cancer.* 2021;20:171. doi:10.1186/s12943-021-01464-x
24. Jorgovanovic D, Song M, Wang L, Zhang Y. Roles of IFN- $\gamma$  in tumor progression and regression: a review. *Biomark Res.* 2020;8:49. doi:10.1186/s40364-020-00228-x
25. Barile L, Vassalli G. Exosomes: therapy delivery tools and biomarkers of diseases. *Pharmacol Ther.* 2017;174:63–78. doi:10.1016/j.pharmthera.2017.02.020
26. Yu X, Odenthal M, Fries JWU. Exosomes as miRNA Carriers: formation–Function–Future. *Int J Mol Sci.* 2016;17:2028. doi:10.3390/ijms17122028
27. Zhang Y, Liu Q, Zhang X, et al. Recent advances in exosome-mediated nucleic acid delivery for cancer therapy. *J Nanobiotechnology.* 2022;20:279. doi:10.1186/s12951-022-01472-z

28. Desgrosellier JS, Cheresh DA. Integrins in cancer: biological implications and therapeutic opportunities. *Nat Rev Cancer*. 2010;10:9–22. doi:10.1038/nrc2748
29. Pina A, Kadri M, Arosio D, et al. Multimeric Presentation of RGD peptidomimetics enhances integrin binding and tumor cell uptake. *Chemistry*. 2020;26:7492–7496. doi:10.1002/chem.202001115
30. Weiss T, Weller M, Roth P. Immunological effects of chemotherapy and radiotherapy against brain tumors. *Expert Rev Anticancer Ther*. 2016;16:1087–1094. doi:10.1080/14737140.2016.1229600
31. Qiao J, Liu Z, Fu Y-X. Adapting conventional cancer treatment for immunotherapy. *J Mol Med*. 2016;94:489–495. doi:10.1007/s00109-016-1393-4
32. Adams S, Diéras V, Barrios CH, et al. Patient-reported outcomes from the Phase III IMpassion130 trial of atezolizumab plus nab-paclitaxel in metastatic triple-negative breast cancer. *Ann Oncol*. 2020;31:582–589. doi:10.1016/j.annonc.2020.02.003

## International Journal of Nanomedicine

Dovepress

### Publish your work in this journal

The International Journal of Nanomedicine is an international, peer-reviewed journal focusing on the application of nanotechnology in diagnostics, therapeutics, and drug delivery systems throughout the biomedical field. This journal is indexed on PubMed Central, MedLine, CAS, SciSearch®, Current Contents®/Clinical Medicine, Journal Citation Reports/Science Edition, EMBase, Scopus and the Elsevier Bibliographic databases. The manuscript management system is completely online and includes a very quick and fair peer-review system, which is all easy to use. Visit <http://www.dovepress.com/testimonials.php> to read real quotes from published authors.

Submit your manuscript here: <https://www.dovepress.com/international-journal-of-nanomedicine-journal>